

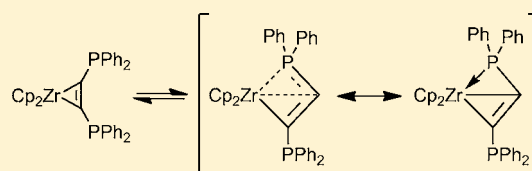
# Synthesis, Characterization and Reactivity of Group 4 Metallocene Bis(diphenylphosphino)acetylene Complexes—A Reactivity and Bonding Study

Martin Haehnel, Sven Hansen, Kathleen Schubert, Perdita Arndt, Anke Spannenberg, Haijun Jiao, and Uwe Rosenthal\*

Leibniz-Institut für Katalyse e.V. an der Universität Rostock, Albert-Einstein-Str. 29a, D-18059 Rostock, Germany

**S** Supporting Information

**ABSTRACT:** A study of the coordination chemistry of bis-(diphenylphosphino)acetylene,  $\text{Ph}_2\text{P}-\text{C}\equiv\text{C}-\text{PPh}_2$ , with selected group 4 metallocenes is presented. By substitution of the alkyne in complexes of the type  $\text{Cp}'_2\text{M}(\text{L})(\eta^2\text{-Me}_3\text{SiC}_2\text{SiMe}_3)$  ( $\text{M} = \text{Ti}$ , no  $\text{L}$ ;  $\text{M} = \text{Zr}$ ,  $\text{L} = \text{pyridine}$ ;  $\text{Cp}' =$  substituted or unsubstituted bridged or unbridged  $\eta^5$ -cyclopentadienyl), the expected mononuclear complexes  $\text{Cp}'_2\text{Ti}(\eta^2\text{-Ph}_2\text{PC}_2\text{PPh}_2)$  (**4Ti**), (*rac*-ebthi) $\text{Ti}(\eta^2\text{-Ph}_2\text{PC}_2\text{PPh}_2)$  (**5Ti**), and (*rac*-ebthi) $\text{Zr}(\eta^2\text{-Ph}_2\text{PC}_2\text{PPh}_2)$  (**5Zr**) [ebthi = ethylenebis(tetrahydroindenyl)] were obtained. When  $[\text{Cp}_2\text{Zr}]$  was used in the reaction of  $\text{Cp}_2\text{Zr}(\text{py})(\eta^2\text{-Me}_3\text{SiC}_2\text{SiMe}_3)$  with  $\text{Ph}_2\text{P}-\text{C}\equiv\text{C}-\text{PPh}_2$ , the dinuclear complex  $[\text{Cp}_2\text{Zr}(\eta^2\text{-Ph}_2\text{PC}_2\text{PPh}_2)]_2$  (**6**) was formed and isolated in the solid state. In solution, this complex is in equilibrium with the very spectacular structure of complex **7b** as the first example of such a highly strained four-membered heterometallacycle of a group 4 metal, involving the rare  $\text{R}_2\text{PCCR}'$  fragment in the cyclic unit. Both the stability and reactivity of heterodisubstituted alkynes  $\text{X}-\text{C}\equiv\text{C}-\text{X}$  ( $\text{X} = \text{NR}_2, \text{PR}_2, \text{SR}, \text{SiR}_3$ , etc.) themselves and also of their complexes are of general interest. Complex **6** did not react with a second  $[\text{Cp}_2\text{Zr}]$  fragment to form a homobimetallic complex. In contrast, for (*rac*-ebthi) $\text{Zr}(\eta^2\text{-Ph}_2\text{PC}_2\text{PPh}_2)$  (**5Zr**) this reaction occurs. In the reaction of complex **4Ti** with the Ni(0) complex  $(\text{Cy}_3\text{P})_2\text{Ni}(\eta^2\text{-C}_2\text{H}_4)$  ( $\text{Cy} = \text{cyclohexyl}$ ), C–P bond cleavage of the alkyne ligand resulted in the formation of the isolated complex  $[(\text{Cy}_3\text{P})\text{Ni}(\mu\text{-PPh}_2)]_2$  (**11**). The structure and bonding of the complexes were investigated by DFT analysis to compare the different possible coordination modes of the  $\text{R}_2\text{P}-\text{C}\equiv\text{C}-\text{PR}_2$  ligand. For compound **7b**, a *flip-flop* coordination of the phosphorus atoms was proposed. Complexes **4Ti**, **5Ti**, **5Zr**, **6**, and **11** were characterized by X-ray crystallography.

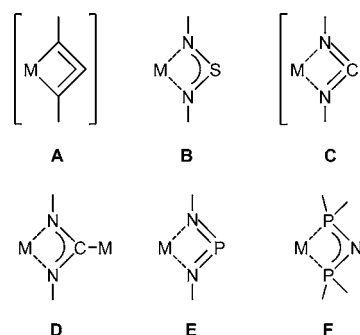


## INTRODUCTION

Unusual highly strained metallacycles have become a well-established part in standard synthetic organometallic chemistry already decades ago.<sup>1</sup> Important to mention are the bis-(trimethylsilyl)acetylene complexes of group 4 metallocenes,  $\text{Cp}'_2\text{M}(\text{L})(\eta^2\text{-Me}_3\text{SiC}_2\text{SiMe}_3)$  ( $\text{Cp}' =$  substituted or unsubstituted  $\eta^5$ -cyclopentadienyl;  $\text{M} = \text{Ti}, \text{Zr}, \text{Hf}$ ;  $\text{L} = \text{THF}, \text{pyridine}, \text{PMe}_3$ ), which serve as excellent precursors for metallocenes to react with other unsaturated substrates by liberating the alkyne unit easily under mild conditions.<sup>2</sup>

While the chemistry of three- and five-membered metallacycles is well-described,<sup>1,3</sup> four-membered highly strained structures were found to be rather difficult to access. Nevertheless, the incorporation of heteroatoms into metallacycles can stabilize highly strained structures.<sup>4,5</sup> Therefore, highly strained four-membered heterometallacycles of group 4 metallocenes have been investigated intensively. It is noteworthy that the all-carbon metallacyclobuta-2,3-dienes (Scheme 1, **A**) were, up to this point, found to be stable only for the group 6 metals tungsten and molybdenum.<sup>6,7</sup> These highly strained complexes result from coupling of a carbyne complex  $[\text{M}\equiv\text{CR}]$  with a terminal alkyne upon deprotonation as a deactivation pathway of the alkyne metathesis catalyst.<sup>7</sup>

## Scheme 1. Different Four-Membered Metallacycles



Contrarily, the reaction of the sulfurdiiimide  $\text{Me}_3\text{SiN}=\text{S}=\text{NSiMe}_3$  with  $\text{Cp}_2\text{M}(\text{L})(\eta^2\text{-Me}_3\text{SiC}_2\text{SiMe}_3)$  ( $\text{Cp} = \eta^5$ -cyclopentadienyl;  $\text{M} = \text{Ti}$ , no  $\text{L}$ ;  $\text{M} = \text{Zr}$ ,  $\text{L} = \text{pyridine}$ ) led to the carbon-free four-membered metallacycles **B** containing nitrogen and sulfur atoms.<sup>8</sup> Using the *N,N*-bis(diphenylphosphino)-amide fragment as a ligand, the formation of the desired four-membered heterometallacycle **F** takes place only if the metal

Received: September 12, 2013

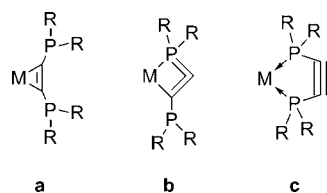
Published: October 24, 2013

center bears a single electron. In fact, the complexes  $Cp_2M(\kappa^2-P_1P_2P_3-C\equiv C-N-PPh_2)$  ( $M = Ti, Zr$ ) are only stable for  $Ti(III)$  and  $Zr(III)$ .<sup>9</sup> Reaction of various carbodiimides  $R-N=C=N-R$  ( $R = i-Pr, t-Bu, Cy, SiMe_3, Mes, Dipp$ ) with  $Cp'_2Ti(\eta^2-Me_3SiC_2SiMe_3)$  ( $Cp' = Cp, Cp^*$ ;  $Cp^* = \eta^5$ -pentamethylcyclopentadienyl) resulted in the formation of the highly strained structure **C**, which attains different modes of stabilization depending on the substituent of the carbodiimide substrate.<sup>10</sup> Exemplarily, the use of cyclohexyl-substituted carbodiimide yielded the metal-stabilized carbene-like metallacycle **D**.<sup>11</sup>

However, complexes of group 4 metallocenes with heterodisubstituted alkynes  $X-C\equiv C-X$  ( $X = Si, N, P, S, B$ ) and heteromonosubstituted alkynes  $R-C\equiv C-X$  ( $X = N, P, S, B$ ) are rarely known. This might be due to the different electronic nature of the substituents, bearing for example a lone pair in case of pnictogens. Therefore, only few such complexes with dipnictogen-substituted alkynes are known, being mostly complexes with nitrogen-substituted alkynes  $R_2N-C\equiv C-NR_2$ .<sup>12</sup> Noteworthy, this class of ligands was studied intensively<sup>12b</sup> on late transition metals such as  $Ru$ .<sup>12c</sup>

Interestingly, there is only one example of a diphosphino-substituted alkyne complex that binds only over the alkyne unit without coordination of the phosphorus atoms (Scheme 2, a).

#### Scheme 2. Proposed Monomolecular Coordination Modes of the $R_2P-C\equiv C-PR_2$ Ligand



This niobium(I) compound,  $(CO)_2I(PPhMe_2)_2Nb(\eta^2-Ph_2PC_2PPh_2)$ , was described by Rehder and co-workers.<sup>16</sup> Furthermore, the incorporation of only one phosphorus atom in the cyclic unit would result in the very interesting coordination mode of a four-membered heterometallacyclobuta-2,3-diene (**b**).

Besides, there are many complexes in which two or even three metal fragments are coordinated to the  $Ph_2P-C\equiv C-PPh_2$  ligand through the triple bond as well as the lone pairs of the phosphorus atoms,<sup>17</sup> thus forming bi- or trimetallic complexes, which include a five-membered heterometallacycle. However, a monomolecular complex displaying this five-membered cycle by coordinating exclusively over the lone pairs of the phosphorus atoms (Scheme 2, c) is unknown up to this point. Noteworthy, there are monophosphino-substituted alkynes that serve as excellent ligands also in case of group 4 metallocene complexes. Tilley and co-workers recently reported on the reactions of  $R_2P-C\equiv C-R'$  ( $R = i-Pr, Et, Ph$ ;  $R' = Ph, Mes$ ) with the zirconocene source  $Cp_2Zr(py)(\eta^2-Me_3SiC_2SiMe_3)$  to give three-membered zirconametallacycloprenes and five-membered zirconametallacyclopentadienes.<sup>14</sup>

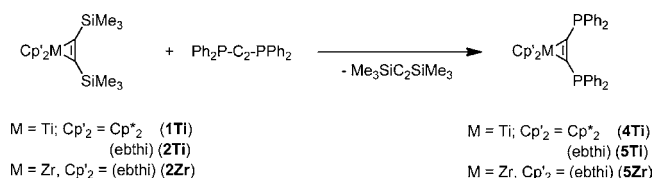
In order to get further insights into the possibility of stabilization by incorporation of only one of the phosphorus atoms (Scheme 2, b), we extended the investigations to the use of the  $Ph_2P-C\equiv C-PPh_2$  ligand for group 4 metallocene complexes. Moreover, it has been found that differently substituted  $\eta^5$ -cyclopentadienyl ligands can influence the chemistry significantly by both steric and electronic

effects.<sup>1,10,18</sup> Therefore, we also elucidated the influence of the  $Cp'_2$  ligand [ $Cp'_2 = Cp_2, Cp^*_2, rac$ -ebthi; ebthi = ethylenebis(tetrahydroindenyl)] on the formation of highly strained heterometallacycles, with the steric demand increasing in the order  $Cp_2 < rac$ -ebthi  $< Cp^*_2$ .

## RESULTS AND DISCUSSION

Reaction of  $Ph_2P-C\equiv C-PPh_2$  with the sterically demanding titanocene source  $Cp^*_2Ti(\eta^2-Me_3SiC_2SiMe_3)$  (**1Ti**) in toluene at elevated temperatures resulted in the alkyne complex  $Cp^*_2Ti(\eta^2-Ph_2PC_2PPh_2)$  (**4Ti**) in very good yields (Scheme 3). When the same reaction was performed with the *ansa*-

#### Scheme 3. Synthesis of Complexes **4Ti**, **5Ti**, and **5Zr**



titanocene alkyne complex **2Ti**, the similar alkyne complex **5Ti** was obtained. Neither **4Ti** nor **5Ti** features any additional coordination of the phosphorus atoms of the ligand, despite the fact that **5Ti** is sterically less crowded than the fully methylated complex **4Ti**. The ligand binds exclusively via the alkyne unit, forming the well-known metallacycloprenene fragment according to coordination mode a in Scheme 2.

The <sup>31</sup>P NMR spectra of these complexes display only one single phosphorus resonance at 7.14 ppm (**4Ti**) and 2.06 ppm (**5Ti**), indicating equivalence of the two phosphorus atoms in solution. The quaternary <sup>13</sup>C signals of the alkyne at 213.4 (**4Ti**) and 213.8 ppm (**5Ti**) appear as doublets as a result of the coupling with the adjacent phosphorus atoms. The coupling constants of 77.5 Hz (**4Ti**) and 76.8 Hz (**5Ti**) are very similar and in the expected range for C–P <sup>1</sup>J couplings. In comparison with the corresponding <sup>13</sup>C NMR signals of **1Ti** and **2Ti** (248.5 and 244.5 ppm, respectively),<sup>19,20</sup> these resonances are significantly shifted upfield. A comparison of the corresponding quaternary <sup>13</sup>C NMR signals of the uncoordinated alkynes ( $Ph_2P-C\equiv C-PPh_2$ , 107.8 ppm;  $Me_3Si-C\equiv C-SiMe_3$ , 114.0 ppm) shows that the resonances of the free ligands are very similar. Therefore, the upfield shifts in complexes **4Ti** and **5Ti** can be attributed to a different binding of the bis-(diphenylphosphino)acetylene to the metal center. In general, the upfield shift indicates a weaker binding of the alkyne to the metal center, leading to more electron density in the C–C multiple bond. However, the lone pairs of the phosphorus atoms might interact with the alkyne unit to transfer electron density into the multiple bond system, leading to an upfield shift in the <sup>13</sup>C NMR spectrum as a result of the hyperconjugation. This observation is in good agreement with the <sup>31</sup>P NMR signals of the phosphorus atoms, which are slightly downfield-shifted compared with the resonance of the free alkyne (–31.6 ppm), indicating this electron transfer. Additionally, the IR spectrum of **4Ti** shows the C=C bond stretch at 1433 cm<sup>–1</sup>, a significant difference (664 cm<sup>–1</sup>) compared with the free ligand (2097 cm<sup>–1</sup>).<sup>21</sup> Therefore, the strong binding of the alkyne unit is similar to that in complex **1Ti**, although the quaternary <sup>13</sup>C NMR resonances are shifted upfield.

The molecular structure of complex **4Ti** is depicted in Figure 1. The titanium center is coordinated by two Cp\* ligands and

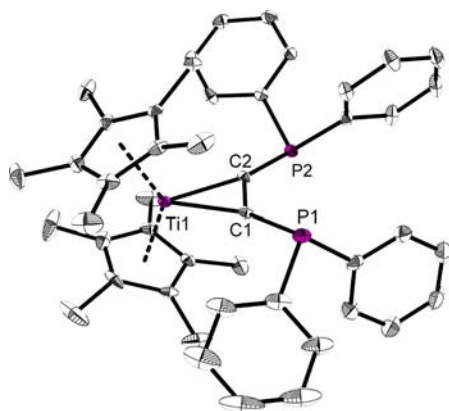


**Figure 1.** Molecular structure of complex **4Ti**. Thermal ellipsoids are drawn at the 30% probability level. The second molecule of the asymmetric unit is structurally similar to the depicted one in terms of bond lengths and angles, and therefore, it is not shown; for full data, see the Supporting Information. Hydrogen atoms have been omitted for clarity. Selected bond lengths [Å] and angles [deg]: Ti1–C1 2.129(2), Ti1–C2 2.115(2), C1–C2 1.317(3); C1–Ti1–C2 36.14(7), P1–C1–C2 131.42(14), C1–C2–P2 134.71(15).

the alkyne unit. The small C1–Ti1–C2 angle of the highly strained three-membered metallacycle is 36.14(7)°. No additional ligand is observed, concerning the steric demand of the Cp\* ligands. Not surprisingly, the Ti–C distances [2.129(2) and 2.115(2) Å] are similar to those of the starting complex **1Ti**.<sup>19</sup> The C–C distance [1.317(3) Å] clearly indicates double-bond character, subsidized by both PCC angles [131.42(14)° and 134.71(15)°], which refer to the sp<sup>2</sup> hybridization of the carbon atoms.

The molecular structure of complex **5Ti** (Figure 2) is very similar to that of complex **4Ti**. Because of the reduced steric

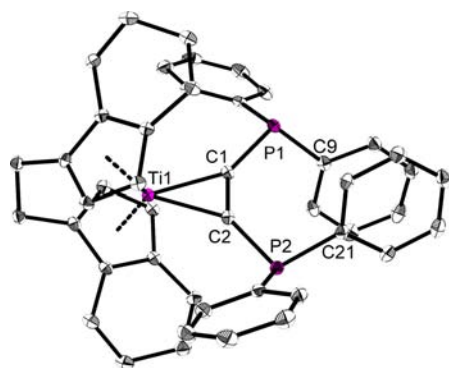


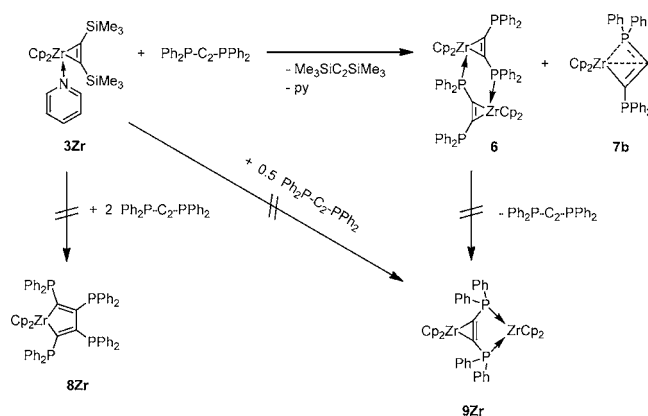
**Figure 2.** Molecular structure of complex **5Ti**. Thermal ellipsoids are drawn at the 30% probability level. Hydrogen atoms have been omitted for clarity. Selected bond lengths [Å] and angles [deg]: Ti1–C1 2.0835(13), Ti1–C2 2.0962(12), C1–C2 1.309(2); C1–Ti1–C2 36.51(5), P1–C1–C2 138.54(10), C1–C2–P2 137.16(10).

demand of the *rac*-ebthi ligand, the titanium carbon distances are even shorter than in complex **4Ti**. The C–C distance [1.309(2) Å] is not significantly different from the distance in **4Ti**, showing the same double-bond character. Remarkably, the Ph groups of C9 and C21 of the ligand are almost parallel (the angle between the planes defined by the two Ph rings is 5.0°),

which indicates  $\pi$ -stacking of these aromatic rings. Furthermore, the centroid–centroid distance is 3.725(1) Å, and the values for the angle between the ring normal and the vector of the ring centroids (22.4 and 26.7°, respectively) are rather large but in good agreement with other  $\pi$ – $\pi$  interactions.<sup>22</sup>

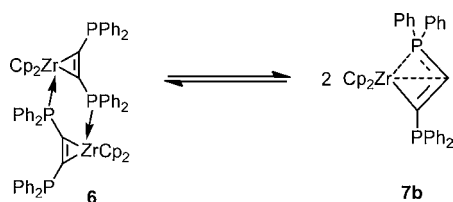
The influence of the Cp ligand as a sterically less demanding substituent was investigated by using Cp<sub>2</sub>Zr(py)( $\eta^2$ -Me<sub>3</sub>SiC<sub>2</sub>SiMe<sub>3</sub>) (**3Zr**). Reaction of **3Zr** with Ph<sub>2</sub>P–C≡C–PPh<sub>2</sub> in noncoordinating solvents yields the dinuclear complex **6** and the mononuclear complex **7b** (Scheme 4). This type of

#### Scheme 4. Synthesis of the Complexes **6** and **7b** and Stoichiometric Variations



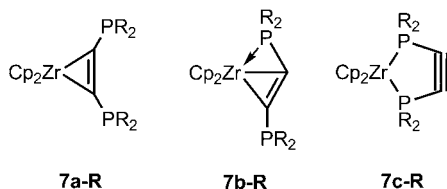
stabilization is known: Tilley and co-workers reported the synthesis of several monosubstituted phosphinoacetylene zirconocene complexes that are also stabilized by intermolecular interactions of the lone pairs of the phosphorus atoms.<sup>14</sup> The dimerization leads to an increase in stability, and it was impossible to prepare the monomeric complex by adding THF or pyridine. Surprisingly, **3Zr** does not react with 2 equiv of alkyne to give a five-membered metallacyclopenta-2,4-diene (**8Zr**). Accordingly, the dinuclear complex **6** does not react with an additional equivalent of alkyne either. These reactions do not occur even at elevated temperature (110 °C). Moreover, the attempt to access the structural motif **9Zr** by reacting two molecules of **3Zr** with one alkyne resulted only in the formation of **6** and **7b**.

In the <sup>31</sup>P NMR spectra of the reaction solution, two different resonances for complex **6** appear at 15.3 and 8.4 ppm, showing the nonequivalent phosphorus atoms. This supports the dimeric nature of complex **6** also in solution. Additionally and most surprisingly, a second set of independent doublets at 12.0 and –15.7 ppm with a P–P coupling constant of <sup>3</sup>J = 190 Hz is present, which can be assigned to the structure of the four membered metallacycle **7b**. The <sup>1</sup>H and <sup>13</sup>C NMR resonances of the Cp rings of complex **6** are in the expected range at 5.52 ppm (<sup>1</sup>H) and 105.8 ppm (<sup>13</sup>C). The second set of signals corresponding to complex **7b** can be found at 5.88 ppm (<sup>1</sup>H) and 111.8 ppm (<sup>13</sup>C). The best **6**:**7b** ratio we could observe was 6:4. Heating of the NMR solution to 75 °C revealed an equilibrium between complexes **6** and **7b** in solution (Scheme 5), but decomposition takes place above 55 °C. Dissolving single crystals of complex **6** in C<sub>6</sub>D<sub>6</sub> also results in equilibration between **6** and **7b** in solution, as in both the <sup>1</sup>H and <sup>31</sup>P NMR spectra the characteristic resonances for **6** and **7b** appear. To the best of our knowledge, complex **7b** is the first example of such a highly strained four-membered heterometallacycle of a

Scheme 5. Observed Equilibrium between Complexes **6** and **7b** in Solution

group 4 metal, involving the rare  $R_2PCCR'$  fragment in the cyclic unit. This is very special because of the electron-deficient character of the Zr center.<sup>4</sup>

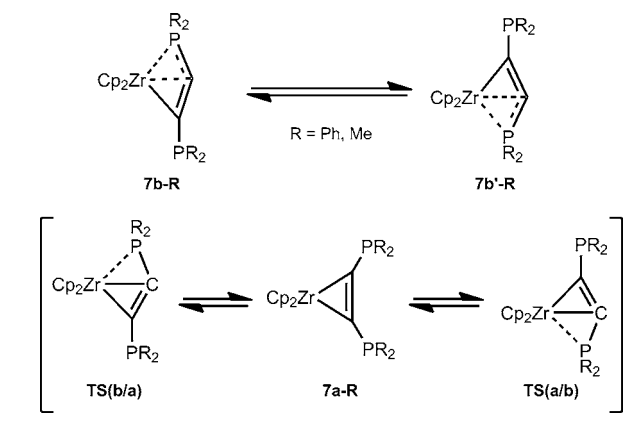
In order to corroborate the experimental results, density functional theory (DFT) calculations were performed. All of the computational details are given in the Supporting Information. It is noted that the optimized structural parameters for complexes **4Ti**, **5Ti**, and **5Zr** are in very good agreement with the data obtained by X-ray crystallography. First we computed the stability of the different coordination modes of bis(phosphine)acetylenes at the  $[Cp_2Zr]$  fragment (Scheme 6) with  $R = Ph$  and Me. At the BP86/TZVP level, the

Scheme 6. Calculated Coordination Isomers of the Monomeric Complex **7-R** ( $R = Ph, Me$ )

three-membered metallacycle **7a-R** is slightly more stable than the four-membered metallacycle **7b-R**. The five-membered metallacycle **7c-R** is not even an energy minimum and is also very high in energy. These results exclude the possible existence of metallacycle **7c** as a stable molecule.

It is very interesting to note that the computed relative energies of **7a-Ph** and **7a-Me** are very close (4.29 and 4.40 kcal/mol, respectively). This rather small energy difference shows that it is reasonable to use methyl substitution to model the phenyl substitution. Since the MP2 method can give more accurate relative energies than BP86 in Zr complexes, we computed MP2 single-point energies on the BP86/TZVP-optimized structures for  $R = Me$ , and the deduced Gibbs free energies show that the four-membered metallacycle **7b-Me** becomes 1.24 kcal/mol more stable than the three-membered metallacycle **7a-Me**. This shows that the free energy difference between **7a-R** and **7b-R** is rather small, thus resulting in the possible existence of both isomeric forms.

The main difference between **6** and **7b** in comparison to complexes **4Ti**, **5Ti**, and **5Zr** is the additional coordination of P, which for **6** arises from an (external) intermolecular P group and for **7b** from an (internal) intramolecular P group. At room temperature, exchange of the coordinating phosphorus atoms of **7b** can be observed by  $^{31}P$  NMR nuclear Overhauser effect spectroscopy (NOESY) (although the cross-peaks are weak; see the Supporting Information), thus indicating a possible dynamic *flip-flop* interaction of the two phosphorus atoms as depicted in Scheme 7. A similar behavior was also found before for Si-H groups in  $Cp_2Ti(\eta^2-HMe_2SiC_2SiMe_2H)$ .<sup>23</sup>

Scheme 7. Possible *Flip-Flop* Interaction of the Two Phosphorus Atoms in **7b-R**

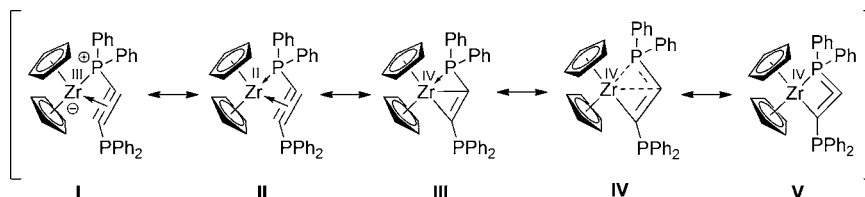
However, in the  $^1H$  NMR NOESY spectrum an additional unclear cross-peak at 5.88 ppm/7.49 ppm was observed. In addition, we computed the *flip-flop* mechanism of the phosphorus atoms proposed for compound **7b-R**. As shown in Scheme 7, the *flip-flop* mechanism between **7b-R** and **7b'-R** involves a two-step pathway. The first step is the dissociation of the coordinating P atom from the central metal atom via the transition state **TS(b/a)** to form the stable three-membered complex **7a**. The second step is the coordination of the other P atom to the central metal atom via the transition state **TS(a/b)** to form the four-membered cycle **7b'-R**. At the BP86/TZVP level, the computed free energy barriers from **7b-R** to **TS(a/b)** are 6.62 kcal/mol for  $R = Ph$  and 6.52 kcal/mol for  $R = Me$ . At the MP2 level for  $R = Me$ , the computed free energy barrier is 14.22 kcal/mol. Since such a *flip-flop* interconversion was observed in the NMR experiment at room temperature, our computed barriers should be reasonable.

The resonance forms, depicted in Scheme 8, are to some extent similar to those for the allenyl/propargylic system of  $Cp_2Zr[\eta^3-C(Ph)=C=CH_2]$  described by Wojcicki and co-workers.<sup>24</sup> In contrast to that work, the phosphorus atom bears an additional electron, which also permits the existence of the metallacycloallene (**V**).

An analysis of the nature of the bonding in complex **7** was conducted. The calculated bond distances for these complexes are shown in Table 1. For  $R = Ph$ , the C=C distance of 1.325 Å in **7b-Ph** is very close to that in **7a-Ph** (1.335 Å). Almost the same trend was also found for complexes **7b-Me** and **7a-Me** (1.328 and 1.339 Å, respectively).

Natural localized molecular orbital (NLMO) analysis favors a metallabicyclobutene complex with a C=C double bond (Scheme 8, **III**) rather than the first-assumed 1-metalla-2-phosphacyclobuta-2,3-diene (**V**) for complex **7b-R**. For example, NLMO reveals double-bond character for the C1–C2 bond and single-bond character for the C2–P2 bond. The computed Wiberg bond indexes (1.908) also show that the C1–C2 bond is indeed a double bond. The bond order for the C2–P2 bond is 0.953, and the bond order for the exocyclic C1–P1 bond is 1.003. Therefore, the best description of the bonding in **7b** would be resonance structure **III**, which corresponds to a metallacyclopentene with the additional intramolecular coordination of the P atom to the free coordination site of the metal as the monomeric form of complex **6**.

Scheme 8. Resonance Forms of Monomeric Complex 7b in Solution

Table 1. BP86-Computed Bond Distances [in Å] in  $\text{Cp}_2\text{Zr}(\text{R}_2\text{P}-\text{C}_2-\text{PR}_2)$ 

	Zr–C1	Zr–C2	C1–C2	C1–P1	C2–P2	Zr–P1
7a-Ph	2.219	2.219	1.335	1.807	1.807	3.871
7b-Ph	2.278	2.493	1.325	1.779	1.826	2.584
TS(b/a) (R = Ph)	2.288	2.242	1.317	1.746	1.817	3.148
7a-Me	2.207	2.207	1.339	1.813	1.813	3.901
7b-Me	2.270	2.468	1.328	1.781	1.815	2.579
TS(b/a) (R = Me)	2.287	2.244	1.315	1.751	1.810	3.157

The molecular structure of complex **6** in the solid state is depicted in Figure 3. The central structural motif is a six-membered ring consisting of two Zr–C–P fragments. Each zirconium center is coordinated by two Cp units, the alkyne fragment, and a phosphorus atom of the second unit of the molecule. As discussed before,<sup>14</sup> this additional coordination is necessary because of both the small steric demand of the Cp ligands and the large size of the zirconium center.

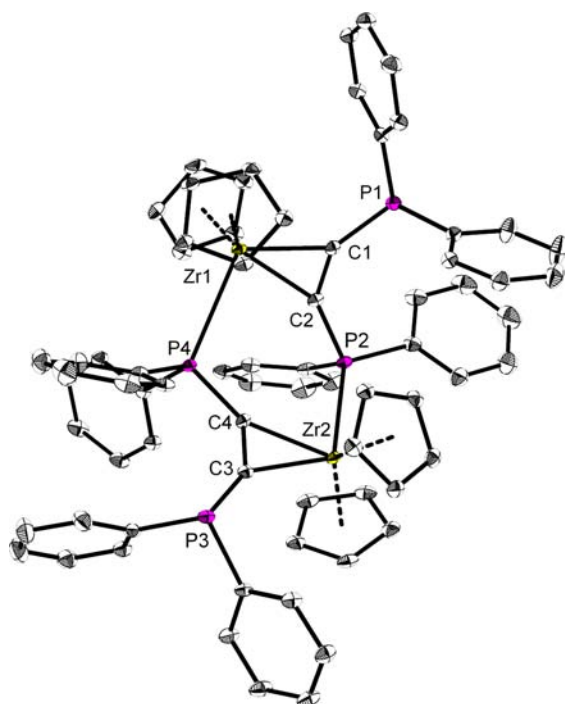


**Figure 3.** Molecular structure of complex **6**. Thermal ellipsoids are drawn at the 30% probability level. Hydrogen atoms and cocrystallized toluene molecules have been omitted for clarity. Selected bond lengths [Å] and angles [deg]: Zr1–C1 2.229(2), Zr1–C2 2.263(2), Zr2–C3 2.232(2), Zr2–C4 2.281(2), C1–C2 1.323(3), C3–C4 1.321(3), Zr1–P4 2.9558(6), Zr2–P2 2.7542(7); C1–Zr1–C2 34.25(8), C3–Zr2–C4 34.01(8), P1–C1–C2 138.8(2), C1–C2–P2 138.4(2), P3–C3–C4 141.7(2), C3–C4–P4 133.6(2).

In order to elucidate the influence of the  $\text{Cp}'_2$  ligand moiety, the reaction of *rac*-ebthi complex **2Zr**, which is sterically more demanding than the  $\text{Cp}_2$  moiety, with  $\text{Ph}_2\text{P}-\text{C}\equiv\text{C}-\text{PPh}_2$  was performed, leading to a more diverse reaction pattern. At room temperature in a 1:1 stoichiometric ratio, the already mentioned substitution reaction of the spectator  $\text{Me}_3\text{Si}-\text{C}\equiv\text{C}-\text{SiMe}_3$  ligand by the  $\text{Ph}_2\text{P}-\text{C}\equiv\text{C}-\text{PPh}_2$  ligand occurs smoothly and results in the formation of the three-membered metallacycle **5Zr** according to Scheme 3. In the  $^{31}\text{P}$  NMR spectrum, the  $^{31}\text{P}$  resonance is found at 3.20 ppm as a singlet, as the two phosphorus atoms are equivalent. The molecular structure of complex **5Zr** is depicted in Figure 4.

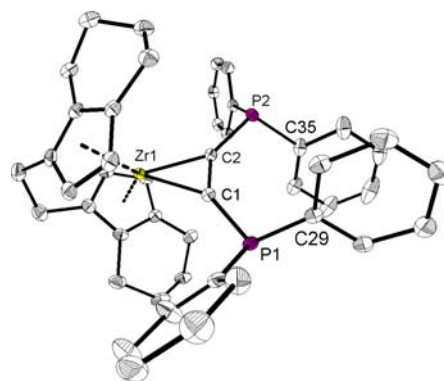
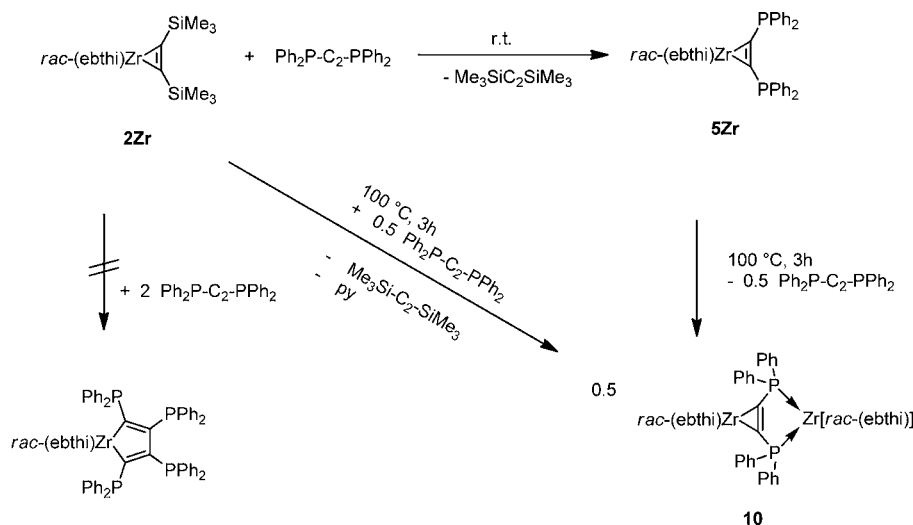


**Figure 4.** Molecular structure of complex **5Zr**. Thermal ellipsoids are drawn at the 30% probability level. Hydrogen atoms, the second orientation of the disordered part of the molecule, and cocrystallized toluene have been omitted for clarity. Selected bond lengths [Å] and angles [deg]: Zr1–C1 2.199(2), Zr1–C2 2.203(2), C1–C2 1.330(3); C1–Zr1–C2 35.17(7), P1–C1–C2 138.53(17), C1–C2–P2 136.16(17).

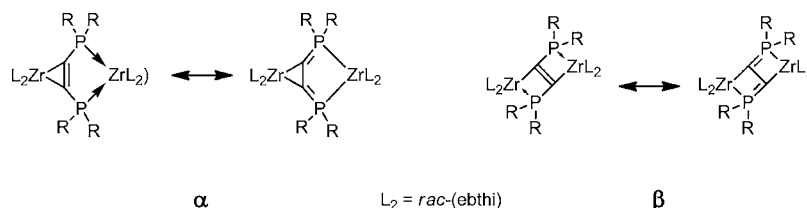
In contrast to complex **6**, no dimerization occurs in the solid state because of the enhanced steric demand of the *rac*-ebthi ligand. A  $\pi$ -stacking interaction like that in **5Ti** is also observed for complex **5Zr**, with a centroid–centroid distance of 3.623(1) Å. It is noteworthy that the ideal  $\pi$ - $\pi$  interaction is found in graphite with a distance of 3.35 Å between the layers.<sup>25</sup> The Ph rings of C29 and C35 are not ideally parallel-oriented, although the angle between the ring planes is rather small (9.5°). The values for the angle between the ring normal and the vector of the ring centroids are 15.8 and 19.5°, respectively.

Upon heating of complex **5Zr** to 100 °C, the color of the reaction mixture slowly changed from dark green to purple. The isolated dark-purple solid (56% yield) can be attributed to the dinuclear complex **10**, according to Scheme 9. A reaction time of 3 h was found to be the optimum, as a longer reaction time led to decomposition of the very unstable complex **10**. Complex **10** is the product of a formal 2:1 metal-to-ligand stoichiometric ratio; the remaining  $\text{Ph}_2\text{P}-\text{C}\equiv\text{C}-\text{PPh}_2$  was identified by both  $^1\text{H}$  and  $^{31}\text{P}$  NMR spectra. When the reaction

Scheme 9. Synthesis of Complex 10 Using Two Different Pathways



Scheme 10. Constitutional Isomers of Complex 10 (R = Ph, Me); Both Resonance Forms of Each Isomer Are Shown



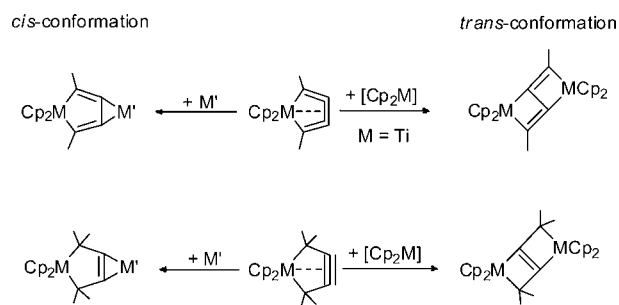
is performed with 2 equiv of **2Zr** and only 1 equiv of  $\text{Ph}_2\text{P}-\text{C}\equiv\text{C}-\text{PPh}_2$  at elevated temperatures, the formation of complex **10** occurs directly. However, this pathway also leads to larger amounts of byproducts. Reaction of **5Zr** with another equivalent of  $\text{Ph}_2\text{P}-\text{C}\equiv\text{C}-\text{PPh}_2$ , representing a 1:2 metal-to-ligand stoichiometric ratio, does not occur.

NMR analysis of complex **10** shows a  $^{31}\text{P}$  NMR resonance at 168.7 ppm, clearly indicating metal coordination of the P atom.<sup>26</sup> Therefore, two possible constitutional isomers  $\alpha$  (cisoid) and  $\beta$  (transoid), together with their resonance forms, are shown in Scheme 10. In the  $^1\text{H}$  NMR spectrum, two sets of *rac*-*ebthi* signals appear. According to these, the most probable structure of complex **10** is postulated to be isomer  $\alpha$ . Additionally, complex **10** was characterized by mass spectrometry. The fragmentation pattern shows the  $[\text{M}-\text{Ph}]$  peak ( $m/z$  1025) and the  $[\text{M}-2\text{Ph}]$  peak ( $m/z$  948).

Unfortunately, complex **10** was found to be very unstable, even in the solid state, and we were not able to get crystals suitable for X-ray analysis to unequivocally corroborate the suggested structure. Therefore, we computed the structure and stability of both possible isomers (Scheme 10). The computed bond distances are listed in the Supporting Information. At the BP86 level, the  $\beta$  isomer is  $C_2$ -symmetric while the  $\alpha$  isomer is  $C_1$ -symmetric. The  $\alpha$  isomer is more stable than the  $\beta$  isomer by 10.02 kcal/mol for R = Ph and 12.00 kcal/mol for R = Me. Even with a simplified model using Cp ligands instead of the *rac*-*ebthi* ligand and R = Me, the  $\alpha$  isomer is more stable than the  $\beta$  isomer by 6.62 kcal/mol. This indicates the higher thermodynamic stability and therefore the preference of the  $\alpha$  isomer over the  $\beta$  isomer, which is in good agreement with the observed data indicating the existence of the  $\alpha$  isomer. It is worth mentioning that analogues for the two possible constitutional isomers  $\alpha$  (cisoid) and  $\beta$  (transoid) were

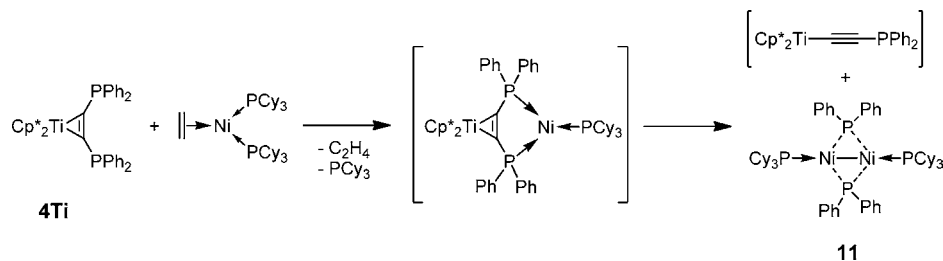
described for the complexation of all-C metallacyclopentynes and -metallacyclocumulenes (Scheme 11).

Scheme 11. Isolated and Characterized Dinuclear Cis and Trans Complexes of All-Carbon Metallacyclocumulenes and Metallacyclopentynes



Complex **4Ti** was reacted with the Ni(0) complex  $(\text{Cy}_3\text{P})_2\text{Ni}(\eta^2-\text{C}_2\text{H}_4)$  (Cy = cyclohexyl)<sup>27</sup> to generate a heterobimetallic complex of an early transition metal and a late transition metal (Scheme 12). Similar bimetallic complexes have been described before for group 4 metals.<sup>17a</sup> The assumed intermediate appears to be even more unstable than complex **10**. In this case, C–P bond cleavage of the alkyne ligand occurs readily, resulting in the formation of the isolated complex **11**. Therefore, this reaction is a good evidence for the existence of both the assumed intermediate and complex **10** as well. A possible mechanism involving complexation of the Ni fragment followed by C–P bond cleavage to give complex **11** is depicted in Scheme 12. Unfortunately, we were unable to identify the second cleavage product, which should contain the titanocene

## Scheme 12. Synthesis of Ni–Ni Complex 11



fragment. However, an oxidation reaction of Ni(0) to Ni(I) occurred.

The molecular structure of complex **11** is depicted in Figure 5. Each Ni atom is surrounded by one coordinating  $\text{PCy}_3$

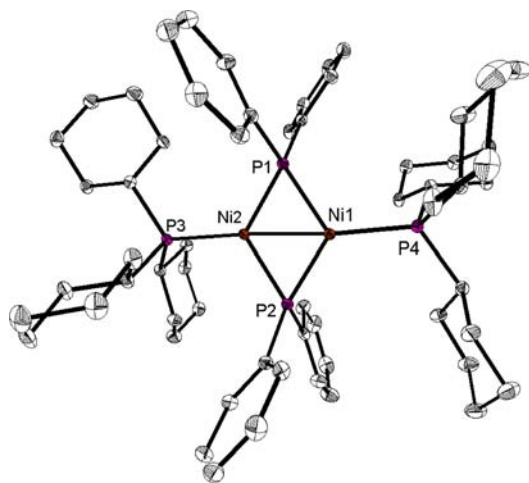


**Figure 5.** Molecular structure of complex **11**. Thermal ellipsoids are drawn at the 30% probability level. Hydrogen atoms and cocrystallized THF molecules have been omitted for clarity. Selected bond lengths [Å] and angles [deg]: P1–Ni1 2.1597(7), P1–Ni2 2.1563(7), P2–Ni1 2.1605(7), P2–Ni2 2.1595(7), P4–Ni1 2.1583(6), P3–Ni2 2.1695(6), Ni1–Ni2 2.3692(4); Ni1–P1–Ni2 66.59(2), Ni1–P2–Ni2 66.52(2).

group, two bridging phosphorus atoms of two  $[\text{Ph}_2\text{P}]^-$  groups, and the second Ni center. Ni1, Ni2, P1, and P2 are almost planar, with the phosphorus atoms P3 and P4 being slightly out of this plane [P3, 0.3752(8) Å above; P4, 0.3985(8) Å below]. All of the P–Ni (P2–Ni, respectively) distances are similar and between 2.1563(7) and 2.1695(6) Å. The Ni1–Ni2 distance [2.3692(4) Å] is in the range of an expected Ni–Ni bond,<sup>28</sup> as found in other complexes displaying this central structural motif.

Such C–E bond cleavage reactions of alkynes  $\text{E}-\text{C}\equiv\text{C}-\text{E}$  have been observed before for various substituents on various metals. Exemplarily, such  $\text{Ph}-\text{C}\equiv\text{C}$  and  $\text{Si}-\text{C}\equiv\text{C}$  bond cleavages are known for Pt complexes.<sup>29,30</sup> Moreover, Si–C cleavages have also been described for the group 4 metals Ti and Hf.<sup>31,32</sup> Cleavage reactions of  $\text{Me}_3\text{SnC}\equiv\text{CSnMe}_3$  and  $\text{PhCH}_2\text{SC}\equiv\text{CSCH}_2\text{Ph}$  have also been described for group 4 metallocene complexes. The stannyl-substituted alkyne complexes  $\text{Cp}'_2\text{Ti}(\eta^2-\text{Me}_3\text{SnC}_2\text{SnMe}_3)$  ( $\text{Cp}' = \text{Cp}, \text{C}_5\text{H}_3\text{Me}_2$ ) were found to be less stable than complex **4Ti**, resulting in Sn–C bond cleavage to give  $[\text{Cp}'_2\text{Ti}(\mu-\eta^2-\eta^1-\text{C}\equiv\text{CSnMe}_3)]_2$ .<sup>33</sup> Moreover, the reaction of  $\text{Cp}_2\text{Ti}(\eta^2-\text{Me}_3\text{SiC}_2\text{SiMe}_3)$  with bis(benzylsulfuryl)acetylene,  $\text{PhCH}_2\text{S}-\text{C}\equiv\text{C}-\text{S}-\text{SCH}_2\text{Ph}$ , yields the complex

$\text{Cp}_2\text{Ti}(\text{SCH}_2\text{Ph})_2$  as well as the dinuclear species  $(\text{Cp}_2\text{Ti})_2(\mu-\kappa^2-\kappa^2-\text{PhCH}_2\text{S}-\text{C}_4-\text{SCH}_2\text{Ph})$  displaying two  $[\text{Cp}_2\text{Ti}]$  moieties bridged by a 1,4-bis(benzylsulfuryl)-1,3-butadiyne in the trans configuration (Scheme 11).<sup>13a</sup>

## CONCLUSION

We have presented a study of the coordination chemistry of bis(diphenylphosphino)acetylene ( $\text{Ph}_2\text{P}-\text{C}\equiv\text{C}-\text{PPh}_2$ ) with selected group 4 metallocenes. This ligand can easily replace the bis(trimethylsilyl)acetylene ligand in complexes of the type  $\text{Cp}'_2\text{M}(\text{L})(\eta^2-\text{Me}_3\text{SiC}_2\text{SiMe}_3)$  to yield the corresponding mononuclear metallacyclopentene complexes. However, depending on the nature of the metallocene moiety, formation of dinuclear complexes can also take place, as was observed for the zirconocene complexes **6** and **10**. In solution, complex **6** was found to be in equilibrium with the mononuclear four-membered metallacycle **7b**, which to the best of our knowledge is the first example of such a highly strained four-membered heterometallacycle of a group 4 metal, involving the rare  $\text{R}_2\text{PCCR}'$  fragment in the cyclic unit. Computational analysis of this species revealed a *flip-flop* coordination of the alkyne ligand at the zirconocene unit, a phenomenon that was described previously for Si–H groups in the titanocene silylalkyne complexes  $\text{Cp}_2\text{Ti}(\eta^2-\text{HMe}_2\text{SiC}_2\text{SiMe}_2\text{H})$ . The barrier for this interconversion for **7b** is rather low, which is in agreement with the observed equilibration at room temperature. As for the bonding in complex **7b**, NLMO analysis suggested a metallabicyclobutene structure to be favored instead of the 1-metalla-2-phosphacyclobuta-2,3-diene. Attempts to generate a heterobimetallic complex of an early transition metal and a late transition metal failed, as rupture of the alkyne ligand took place in the reaction of **4Ti** and the Ni(0) complex  $(\text{Cy}_3\text{P})_2\text{Ni}(\eta^2-\text{C}_2\text{H}_4)$ . However, the structure of the isolated product **11** points toward the intermediacy of the desired heterobimetallic Ti–Ni complex. The present results are essential for an understanding of the coordination chemistry of heteroatom-substituted alkynes at early-transition-metal centers. Further studies to understand the characteristics and to extend the scope of the herein-described unprecedented four-membered heterometallacycle **7b** are underway in our group.

## EXPERIMENTAL DETAILS

**General Information.** All manipulations were carried out under an oxygen- and moisture-free argon atmosphere using standard Schlenk and drybox techniques. Non-halogenated solvents were dried over sodium/benzophenone and freshly distilled prior to use. The metallocene bis(trimethylsilyl)acetylene complexes were synthesized as described previously in the literature.<sup>2</sup> The following instruments were used: NMR spectra: Bruker AV300 and AV400 spectrometers; <sup>1</sup>H and <sup>13</sup>C chemical shifts were referenced to the benzene-*d*<sub>6</sub> solvent signals ( $\delta_{\text{H}}$  7.16,  $\delta_{\text{C}}$  128.0). IR: Bruker Alpha FT-IR spectrometer. MS:

Finnigan MAT 95-XP instrument (Thermo Electron). Elemental analysis: Leco Tru Spec elemental analyzer. Melting points: Mettler-Toledo MP 70 apparatus; melting points are uncorrected and were measured in sealed capillaries.

**Computational Details.** Our computations were carried out at the BP86<sup>34</sup> level of density functional theory as implemented in the Gaussian 09 program,<sup>35</sup> and all of the computational details are given in the Supporting Information. For geometry optimizations, we used the SVP<sup>36</sup> and TZVP<sup>37</sup> basis sets for all nonmetal elements (C, H, and P) and the LANL2DZ<sup>38</sup> basis set for Ti and Zr (BP86/SVP and BP86/TZVP, respectively). All of the optimized structures were characterized either as energy minima without imaginary frequencies or transition states with only one imaginary frequency by frequency calculations at the same level. The computed Gibbs free energies ( $\Delta G$ ) at 298 K deduced from the frequency calculations were used for discussion and comparison. In addition, we computed MP2 single-point energies on the BP86/TZVP-optimized geometries. In our previous benchmark studies for Ti, Zr, and Hf chemistry,<sup>39</sup> we found that BP86/TZVP can give not only reasonable geometries but also the right relative energies for titanocene chemistry, and even more accurate energetic orders for the different structural isomers of these metal complexes have been found at the MP2 level.

**Syntheses.**  $Cp^*_2Ti(\eta^2-Ph_2PC_2PPh_2)$  (**4Ti**). To a stirred solution of 1Ti (662 mg, 1.35 mmol) in 10 mL of toluene was added a solution of  $Ph_2P-C\equiv C-PPh_2$  (534 mg, 1.35 mmol) in 10 mL of toluene. After the reaction mixture was stirred for 24 h at 65 °C, the color changed from light brown to dark green. The mixture was cooled to room temperature, and all volatiles were removed in vacuum. The dark-green residue was dissolved in 10 mL of *n*-hexane and stored at -78 °C for 3 days. The emerald-green precipitate was filtered, washed with cold *n*-hexane, and dried in vacuum. Crystals suitable for X-ray analysis were obtained from a saturated solution of *n*-hexane at room temperature. Yield: 761 mg (79%). Mp: 159 °C (dec., under Ar). NMR (benzene-*d*<sub>6</sub>, 300 MHz, 296 K): <sup>1</sup>H:  $\delta$  7.05–6.97 (m), 20H; 1.83 (s), 30H (Me). <sup>13</sup>C:  $\delta$  213.4 (d, <sup>1</sup>J = 77.5 Hz); 140.4 (m); 133.9 (m); 129.3 (s); 127.8 (t, <sup>4</sup>J = 3.1 Hz); 125.0 (s) (Cp\*); 13.3 (s, Me). <sup>31</sup>P{<sup>1</sup>H}:  $\delta$  7.1. Anal. Calcd for C<sub>46</sub>H<sub>40</sub>P<sub>2</sub>Ti: C, 77.52; H, 7.07%. Found: C, 77.34; H, 7.02%. MS (CI, *i*-butane) *m/z*: 712 [M]<sup>+</sup>, 527 [M - PPh<sub>2</sub>]<sup>+</sup>, 318 [Cp\*<sub>2</sub>Ti]<sup>+</sup>.

$[rac\text{-Ethylenebis}(\eta^2\text{-}1,1'\text{-tetrahydroindenyl})]Ti(\eta^2\text{-}Ph_2PC_2PPh_2)$  (**5Ti**). To a stirred solution of 2Ti (210 mg, 0.44 mmol) in 10 mL of toluene was added a solution of  $Ph_2P-C\equiv C-PPh_2$  (172 mg, 0.44 mmol) in 10 mL of toluene at -40 °C. After 1 h of stirring at -40 °C, the solution was allowed to warm to room temperature and then heated for 3 days at 60 °C, turning the color of the reaction mixture from brown to dark brown. After the mixture was cooled to room temperature, all of the volatiles were removed in vacuum, and the resulting dark-brown precipitate was slurried in 20 mL of *n*-hexane and 7 mL of THF, filtered, and stored at -78 °C for 7 days. The dark-brown precipitate was filtered again, and the solution was stored at room temperature overnight to give dark-green crystals of 5Ti, which were filtered and dried in vacuum. Yield: 201 mg (65%). Mp: 142 °C (dec., under Ar). NMR (benzene-*d*<sub>6</sub>, 300 MHz, 296 K): <sup>1</sup>H:  $\delta$  7.53–7.49 (m), 4H (*o*-Ph); 7.45 (d, <sup>2</sup>J = 3.2 Hz), 2H (Cp); 7.19–7.46 (m), 6H (*m*-Ph, *p*-Ph); 6.93–6.89 (m), 6H (*m*-Ph, *p*-Ph); 6.48–6.44 (m), 4H (*o*-Ph); 4.60 (d, <sup>2</sup>J = 3.2 Hz), 2H (Cp); 3.93–3.91 (m), 2H; 3.24–3.20 (m), 2H; 2.33–2.29 (m), 4H (CH<sub>2</sub>); 1.79–1.75 (m), 4H (CH<sub>2</sub>); 1.45–1.42 (m), 4H (CH<sub>2</sub>); 1.22–1.19 (m), 4H (CH<sub>2</sub>). <sup>13</sup>C:  $\delta$  213.8 (d, <sup>1</sup>J = 76.8 Hz); 142.2 (t, <sup>1</sup>J = 4.7 Hz); 138.5 (t, <sup>1</sup>J = 7.4 Hz); 129.3 (s); 135.7 (t, <sup>2</sup>J = 12.0 Hz); 132.1 (t, <sup>2</sup>J = 8.2 Hz); 129.7; 128.6; 127.9; 127.5 (t, <sup>2</sup>J = 2.6 Hz); 127.0; 126.6; 126.1; 117.6; 113.7; 26.8; 26.0; 25.9; 23.9; 23.7; 23.0; 13.3 (s, Me). <sup>31</sup>P{<sup>1</sup>H}:  $\delta$  2.1. Anal. Calcd for C<sub>46</sub>H<sub>44</sub>P<sub>2</sub>Ti: C, 78.18; H, 6.28%. Found: C, 77.91; H, 6.63%. MS (EI) *m/z*: 264 [rac-ebthi]<sup>+</sup>, 185 [PPh<sub>2</sub>]<sup>+</sup>.

$[Cp_2Zr(\eta^2-Ph_2PC_2PPh_2)]_2$  (**6**). To a stirred solution of 3Zr (350 mg, 0.743 mmol) in 15 mL of toluene was added a solution of  $Ph_2P-C\equiv C-PPh_2$  (293 mg, 0.743 mmol) in 10 mL of toluene at -40 °C. While the reaction mixture was allowed to warm to room temperature, the color turned from gray to dark orange. After an additional 18 h of stirring, all of the volatiles were removed in vacuum, and the resulting

dark-orange precipitate was dissolved in 20 mL of toluene and filtered. The resulting solution was concentrated to ca. 10 mL and stored at -40 °C to yield a dark-yellow precipitate after 7 days; the precipitate was filtered, washed with cold toluene, and dried in vacuum. Crystals suitable for X-ray analysis were obtained from a saturated solution of toluene at room temperature. In solution, there was spectroscopic evidence for the formation of complex 7b.

Data for complex 6: Yield: 289 mg (63%). Mp: 68 °C (dec., under Ar). NMR (benzene-*d*<sub>6</sub>, 300 MHz, 296 K): <sup>1</sup>H:  $\delta$  7.69–7.64 (m), 16H; 7.58–7.50 (m), 8H; 7.11–6.89 (m), 16H; 5.52 (s), 20H. <sup>13</sup>C:  $\delta$  135.4; 134.3; 133.4; 131.0; 129.8, 128.9; 125.6; 119.5; 105.8. <sup>31</sup>P{<sup>1</sup>H}:  $\delta$  15.4 (dd, *J* = 8.5 Hz, *J* = 3.6 Hz); 8.4 (dd, *J* = 8.5 Hz, *J* = 3.6 Hz). Anal. Calcd for C<sub>72</sub>H<sub>60</sub>P<sub>4</sub>Zr<sub>2</sub>·2 toluene: C, 72.95; H, 5.41%. Found: C, 73.69; H, 5.09%. MS (EI) *m/z*: 429 [(M/2) - PPh<sub>2</sub>]<sup>+</sup>, 394 [(M/2) - Cp<sub>2</sub>Zr]<sup>+</sup>, 185 [PPh<sub>2</sub>]<sup>+</sup>.

NMR data for complex 7b: <sup>1</sup>H:  $\delta$  7.77 (t, <sup>3</sup>J = 7.1 Hz), 8H (Ph); 7.58–7.53 (m), 4H; 7.43–7.41 (m), 2H; 7.21–7.14 (m), 6H; 5.88 (s), 10H (Cp). <sup>13</sup>C:  $\delta$  111.8 (Cp). Because of the complicated spectrum, no other resonances could be assigned with certainty, as these could also be part of the set of resonances for complex 6. <sup>31</sup>P{<sup>1</sup>H}:  $\delta$  12.0 (d, *J* = 190.2 Hz); -15.72 (d, *J* = 190.2 Hz).

$[rac\text{-Ethylenebis}(\eta^2\text{-}1,1'\text{-tetrahydroindenyl})]Zr(\eta^2\text{-}Ph_2PC_2PPh_2)$  (**5Zr**). To a stirred solution of 2Zr (263 mg, 0.500 mmol) in 15 mL of toluene was added a solution of  $Ph_2P-C\equiv C-PPh_2$  (197 mg, 0.500 mmol) in 10 mL of toluene at 25 °C. After 6 h of stirring, the reaction mixture turned from gray to dark green. An additional 3 days of stirring led to completion of the reaction. After removal of all volatiles in vacuum, the resulting dark-green precipitate was dissolved in 10 mL of toluene and filtered. The dark-green solution was stored at -78 °C to yield a dark-green precipitate after 3 days; the precipitate was filtered, washed with cold toluene, and dried in vacuum. Crystals suitable for X-ray analysis were obtained from a saturated solution of toluene at room temperature. Yield: 265 mg (71%). Mp: 140 °C (dec., under Ar). NMR (benzene-*d*<sub>6</sub>, 300 MHz, 296 K): <sup>1</sup>H:  $\delta$  7.53–7.48 (m), 4H (*o*-Ph); 7.21–7.06 (m), 8H (Ph); 7.05–6.93 (m), 8H (Ph); 6.72 (d, <sup>2</sup>J = 6.0 Hz), 2H (Cp); 5.05 (d, <sup>2</sup>J = 6.0 Hz), 2H (Cp); 3.62–3.53 (m), 2H; 2.87–2.77 (m), 2H; 2.34–2.22 (m), 2H; 1.81–1.72 (m), 2H; 1.65–1.54 (m), 4H; 1.50–1.24 (m), 8H. <sup>13</sup>C:  $\delta$  144.0; 135.3; 135.2; 132.6 (t, *J* = 8.1 Hz); 129.8; 128.9; 128.8; 126.7 (d, *J* = 4.2 Hz); 125.7; 125.3; 124.7; 111.9; 110.8; 27.1; 25.5; 24.0; 23.2. <sup>31</sup>P{<sup>1</sup>H}:  $\delta$  3.2. Anal. Calcd for C<sub>46</sub>H<sub>44</sub>P<sub>2</sub>Zr: C, 73.66; H, 5.91%. Found: C, 73.61; H, 6.30%. MS (EI) *m/z*: 749 [M + H]<sup>+</sup>, 394 [M - (rac-ebthi)Zr]<sup>+</sup>, 264 [(rac-ebthi)]<sup>+</sup>.

$[rac\text{-Ethylenebis}(\eta^5\text{-}1,1'\text{-tetrahydroindenyl})]Zr(\mu_2\text{-}\sigma^2\text{-}Ph_2PC_2PPh_2\text{-}P,P')Zr[rac\text{-ethylenebis}(\eta^2\text{-}1,1'\text{-tetrahydroindenyl})]$  (**10**). Complex 5Zr (265 mg, 0.353 mmol) was dissolved in 15 mL of toluene. While the reaction mixture was stirred at 100 °C for 3 h, the color of the mixture changed from dark blue to purple. After the mixture was cooled to room temperature, all of the volatiles were removed in vacuum, and the resulting dark-purple precipitate was suspended in 35 mL of *n*-hexane. After filtration from the insoluble  $Ph_2P-C\equiv C-PPh_2$ , the purple solution was stored at -78 °C to yield a dark-purple solid, which was filtered, washed with cold *n*-hexane, and dried in vacuum. Yield: 109 mg (56%). Mp: 76 °C (dec., under Ar). NMR (benzene-*d*<sub>6</sub>, 300 MHz, 296 K): <sup>1</sup>H:  $\delta$  7.99–7.91 (m), 8H (Ph); 7.72–7.65 (m), 8H (Ph); 7.56–7.51 (m), 4H (Ph); 6.37 (d, <sup>2</sup>J = 3.0 Hz), 2H (Cp); 5.99 (dd, *J* = 8.8 Hz, *J* = 3.0 Hz), 2H (Cp); 5.74 (d, *J* = 3.0 Hz), 2H (Cp); 5.39 (d, *J* = 3.0 Hz), 2H (Cp); 3.29–3.17 (m), 2H; 2.85–2.27 (m), 2H; 1.98–1.73 (m), 8H; 1.46–1.29 (m), 8H. <sup>13</sup>C:  $\delta$  134.2; 133.4; 133.2; 133.0; 132.1; 130.3; 130.0; 128.8; 128.5; 128.1; 127.9; 127.1; 111.8; 103.9; 31.9; 28.8; 27.7; 24.9; 24.7; 23.0; 22.9; 16.1; 14.3. <sup>31</sup>P{<sup>1</sup>H}:  $\delta$  168.7. Anal. Calcd for C<sub>66</sub>H<sub>68</sub>P<sub>4</sub>Zr<sub>2</sub>: C, 71.70; H, 6.20%. Found: C, 71.05; H, 6.43%. MS (EI) *m/z*: 1025 [M - Ph]<sup>+</sup>, 948 [M - 2Ph]<sup>+</sup>, 264 [(rac-ebthi)]<sup>+</sup>.

$[Cy_3PnI(\mu\text{-}PPh_2)]_2$  (**11**). To a stirred solution of 4Ti (400 mg, 0.561 mmol) in 20 mL of THF was added a solution of  $(\eta^2\text{-}C_2H_4)_2Ni(P\text{-}(C_6H_{11})_3)_2$  (364 mg, 0.561 mmol) in 15 mL of THF at 25 °C. After 16 h of stirring, the reaction mixture turned from green to dark brown. After removal of all volatiles in vacuum, the resulting dark-brown precipitate was dissolved in a mixture of 15 mL of toluene and 15 mL

of THF and filtered. The dark-brown solution was stored at +8 °C to yield dark-brown crystals after 3 weeks; the crystals were filtered, washed with cold toluene, and dried in vacuum. Yield: 29 mg (5%). Unfortunately, because of the low yield, no melting point or elemental analysis could be performed. NMR (benzene-*d*<sub>6</sub>, 300 MHz, 296 K): <sup>1</sup>H: δ 7.06–6.95 (m), 20H (Ph); 1.70–0.98 (m), 66H (Cy). Because of the low concentration of the sample, no meaningful <sup>13</sup>C NMR spectrum could be obtained. <sup>31</sup>P{<sup>1</sup>H}: δ 45.9; 10.3. MS (EI) *m/z*: 280 [PCy<sub>3</sub>]<sup>+</sup>, 185 [PPPh<sub>2</sub>]<sup>+</sup>.

## ■ ASSOCIATED CONTENT

### ■ Supporting Information

Crystallographic data for complexes **4Ti**, **5Ti**, **5Zr**, **6**, and **11** in CIF format; NMR spectra; and details of the DFT calculations. This material is available free of charge via the Internet at <http://pubs.acs.org>.

## ■ AUTHOR INFORMATION

### Corresponding Author

E-mail: [uwe.rosenthal@catalysis.de](mailto:uwe.rosenthal@catalysis.de), Phone: +49 381 1281 176; Fax: +49 381 1281 51176.

### Notes

The authors declare no competing financial interest.

## ■ ACKNOWLEDGMENTS

Dedicated to Professor Dietmar Seyferth on occasion of his 85th birthday on 11th of January 2014. We thank our technical and analytical staff for assistance, in particular PD Dr. Wolfgang Baumann for help with the interpretation of the NMR spectra. Financial support by the DFG (RO 1269/8-1) is gratefully acknowledged. We are thankful to the reviewers for their valuable comments.

## ■ REFERENCES

- (1) Rosenthal, U.; Burlakov, V. V.; Arndt, P.; Baumann, W.; Spannenberg, A. *Organometallics* **2003**, *22*, 884.
- (2) (a) Rosenthal, U.; Burlakov, V. V.; Bach, M. A.; Beweries, T. *Chem. Soc. Rev.* **2007**, *36*, 719. (b) Beweries, T.; Rosenthal, U. Group 4 Metallocene Complexes with Bis(trimethylsilyl)acetylene. In *Science of Synthesis Knowledge Updates 2011/4*; Hall, D. G., Ishihara, K., Li, J. J., Marek, I., North, M., Schaumann, E., Weinreb, S. M., Yus, M., Vol. Eds.; Thieme: Stuttgart, Germany, 2011.
- (3) Rosenthal, U.; Burlakov, V. V.; Arndt, P.; Baumann, W.; Spannenberg, A. *Organometallics* **2005**, *24*, 456.
- (4) Roy, S.; Jemmis, E. D.; Schulz, A.; Beweries, T.; Rosenthal, U. *Angew. Chem., Int. Ed.* **2012**, *51*, 5347.
- (5) Lamac, M.; Spannenberg, A.; Jiao, H.; Hansen, S.; Baumann, W.; Arndt, P.; Rosenthal, U. *Angew. Chem., Int. Ed.* **2010**, *49*, 2937.
- (6) (a) McCullough, L. G.; Listemann, M. L.; Schrock, R. R.; Churchill, M. R.; Ziller, J. W. *J. Am. Chem. Soc.* **1983**, *105*, 6729. (b) McCullough, L. G.; Schrock, R. R.; Dewan, J. C.; Murdzek, J. C. *J. Am. Chem. Soc.* **1985**, *107*, 5987.
- (7) Heppekaussen, J.; Stade, R.; Kondoh, A.; Seidel, G.; Goddard, R.; Fürstner, A. *Chem.—Eur. J.* **2012**, *18*, 10281.
- (8) Kaleta, K.; Ruhmann, M.; Theilmann, O.; Roy, S.; Beweries, T.; Arndt, P.; Villinger, A.; Jemmis, E. D.; Schulz, A.; Rosenthal, U. *Eur. J. Inorg. Chem.* **2012**, 611.
- (9) Haehnel, M.; Hansen, S.; Spannenberg, A.; Arndt, P.; Beweries, T.; Rosenthal, U. *Chem.—Eur. J.* **2012**, *18*, 10546.
- (10) Haehnel, M.; Ruhmann, M.; Theilmann, O.; Roy, S.; Beweries, T.; Arndt, P.; Spannenberg, A.; Villinger, A.; Jemmis, E. D.; Schulz, A.; Rosenthal, U. *J. Am. Chem. Soc.* **2012**, *134*, 15979.
- (11) Theilmann, O.; Ruhmann, M.; Villinger, A.; Schulz, A.; Seidel, W. W.; Kaleta, K.; Beweries, T.; Arndt, P.; Rosenthal, U. *Angew. Chem., Int. Ed.* **2010**, *49*, 9282.

- (12) (a) Tamm, M. Private communication, unpublished results. (b) Petrov, A. R.; Daniliuc, C. G.; Jones, P. G.; Tamm, M. *Chem.—Eur. J.* **2010**, *16*, 11804. (c) Petrov, A. R.; Bannenberg, T.; Daniliuc, C. G.; Jones, P. G.; Tamm, M. *Dalton Trans.* **2011**, *40*, 10503.
- (13) (a) Altenburger, K.; Semmler, J.; Arndt, P.; Spannenberg, A.; Villinger, A.; Seidel, W. W.; Rosenthal, U. *Eur. J. Inorg. Chem.* **2013**, 4258. (b) Altenburger, K.; Arndt, P.; Spannenberg, A.; Baumann, W.; Rosenthal, U. *Eur. J. Inorg. Chem.* **2013**, 3200.
- (14) Müller, A. D.; Johnson, S. A.; Tupper, K. A.; McBee, J. L.; Tilley, T. D. *Organometallics* **2009**, *28*, 1252.
- (15) Xu, X.; Frohlich, R.; Daniliuc, C. G.; Kehr, G.; Erker, G. *Chem. Commun.* **2012**, 48, 6109.
- (16) Rodewald, D.; Schulzke, C.; Rehder, D. *J. Organomet. Chem.* **1995**, *498*, 29.
- (17) (a) Powell, A. K.; Went, M. J. *J. Chem. Soc., Dalton Trans.* **1992**, 439. (b) Hong, F.-E.; Chang-Chang, C. P.; Chang, R.-E.; Chen, S.-C.; Ko, B.-T. *Organometallics* **2002**, *21*, 961.
- (18) Beweries, T.; Haehnel, M.; Rosenthal, U. *Catal. Sci. Technol.* **2013**, *3*, 18.
- (19) Burlakov, V. V.; Polyakov, A. V.; Yanovsky, A. I.; Struchkov, Y. T.; Shur, V. B.; Vol'pin, M. E.; Rosenthal, U.; Görls, H. *J. Organomet. Chem.* **1994**, *476*, 197.
- (20) Lefeber, C.; Baumann, W.; Tillack, A.; Kempe, R.; Görls, H.; Rosenthal, U. *Organometallics* **1996**, *15*, 3486.
- (21) King, R. B.; Efraty, A. *Inorg. Chim. Acta* **1970**, *4*, 319.
- (22) Janiak, C. *J. Chem. Soc., Dalton Trans.* **2000**, 3885.
- (23) Ohff, A.; Kosse, P.; Baumann, W.; Tillack, A.; Kempe, R.; Görls, H.; Burlakov, V. V.; Rosenthal, U. *J. Am. Chem. Soc.* **1995**, *117*, 10399.
- (24) Blosser, P. W.; Gallucci, J. C.; Wojcicki, A. *J. Am. Chem. Soc.* **1993**, *115*, 2994.
- (25) Delhaes, P. *Graphite and Precursors*; CRC Press: Boca Raton, FL, 2001.
- (26) Baker, R. T.; Whitney, J. F.; Wreford, S. S. *Organometallics* **1983**, *2*, 1049.
- (27) Wilke, G.; Herrmann, G. *Angew. Chem., Int. Ed. Engl.* **1962**, *1*, 549.
- (28) Kriley, C. E.; Woolley, C. J.; Krepps, M. K.; Popa, E. M.; Fanwick, P. E.; Rothwell, I. P. *Inorg. Chim. Acta* **2000**, 300–302, 200.
- (29) Müller, C.; Iverson, C. N.; Lachicotte, R. J.; Jones, W. D. *J. Am. Chem. Soc.* **2001**, *123*, 9718.
- (30) Müller, C.; Lachicotte, R. J.; Jones, W. D. *Organometallics* **2002**, *21*, 1190.
- (31) Arndt, P.; Baumann, W.; Spannenberg, A.; Rosenthal, U.; Burlakov, V. V.; Shur, V. B. *Angew. Chem., Int. Ed.* **2003**, *42*, 1414.
- (32) Beweries, T.; Burlakov, V. V.; Bach, M. A.; Peitz, S.; Arndt, P.; Baumann, W.; Spannenberg, A.; Rosenthal, U.; Pathak, B.; Jemmis, E. D. *Angew. Chem., Int. Ed.* **2007**, *46*, 6907.
- (33) Varga, V.; Mach, K.; Hiller, J.; Thewalt, U.; Sedmera, P.; Polasek, M. *Organometallics* **1995**, *14*, 1410.
- (34) Perdew, J. P. *Phys. Rev. B* **1986**, *33*, 8822.
- (35) Frisch, M. J.; Trucks, G. W.; Schlegel, H. B.; Scuseria, G. E.; Robb, M. A.; Cheeseman, J. R.; Scalmani, G.; Barone, V.; Mennucci, B.; Petersson, G. A.; Nakatsuji, H.; Caricato, M.; Li, X.; Hratchian, H. P.; Izmaylov, A. F.; Bloino, J.; Zheng, G.; Sonnenberg, J. L.; Hada, M.; Ehara, M.; Toyota, K.; Fukuda, R.; Hasegawa, J.; Ishida, M.; Nakajima, T.; Honda, Y.; Kitao, O.; Nakai, H.; Vreven, T.; Montgomery, J. A., Jr.; Peralta, J. E.; Ogliaro, F.; Bearpark, M.; Heyd, J. J.; Brothers, E.; Kudin, K. N.; Staroverov, V. N.; Kobayashi, R.; Normand, J.; Raghavachari, K.; Rendell, A.; Burant, J. C.; Iyengar, S. S.; Tomasi, J.; Cossi, M.; Rega, N.; Millam, N. J.; Klene, M.; Knox, J. E.; Cross, J. B.; Bakken, V.; Adamo, C.; Jaramillo, J.; Gomperts, R.; Stratmann, R. E.; Yazyev, O.; Austin, A. J.; Cammi, R.; Pomelli, C.; Ochterski, J. W.; Martin, R. L.; Morokuma, K.; Zakrzewski, V. G.; Voth, G. A.; Salvador, P.; Dannenberg, J. J.; Dapprich, S.; Daniels, A. D.; Farkas, Ö.; Foresman, J. B.; Ortiz, J. V.; Cioslowski, J.; Fox, D. J. *Gaussian 09*, revision C.01; Gaussian, Inc.: Wallingford, CT, 2010.
- (36) Schäfer, A.; Horn, H.; Ahlrichs, R. *J. Chem. Phys.* **1992**, *97*, 2571.
- (37) Schäfer, A.; Huber, C.; Ahlrichs, R. *J. Chem. Phys.* **1994**, *100*, 5829.

- (38) Hay, P. J.; Wadt, W. R. *J. Chem. Phys.* **1985**, *82*, 299.
- (39) Lamač, M.; Spannenberg, A.; Baumann, W.; Fischer, C.; Jiao, H.; Hansen, S.; Arndt, P.; Rosenthal, U. *J. Am. Chem. Soc.* **2010**, *132*, 4369.